Granular Matter (2019) 21:56
https://doi.org/10.1007/s10035-019-0910-x

ORIGINAL PAPER

Packing and flow profiles of soft grains in 3D silos reconstructed with X-ray computed tomography

Ralf Stannarius[1] · Diego Sancho Martinez[1] · Tilo Finger[1] · Ellák Somfai[2] · Tamás Börzsönyi[2]

Received: 22 February 2019 / Published online: 15 June 2019

Abstract
The outflow of hard grains from storage containers with narrow outlets has been extensively studied in the past. Most experiments focused on discharge rates and avalanche statistics. Flow fields inside such containers have been detected optically in two-dimensional (2D) or quasi-2D geometries. Soft grains behave qualitatively different in many respects, both in their static packing properties and during silo discharge. We employ X-ray computed tomography to map the particles in a 3D container and we compare the static packing characteristics and the flow profiles of soft hydrogel spheres with those of hard spheres. The local fill fraction of the soft grains depends upon the depth below the granular surface. The outflow of the soft, low frictional hydrogel spheres involves the complete container volume, stagnant zones are absent.

Keywords Soft grains · X-ray computed tomography · Silo discharge

1 Introduction

Granular materials are ubiquitous, we encounter them in daily routine, and their storage and handling have played an important role in human culture for millennia. It is therefore quite remarkable that the quantitative physical understanding of packing and flow processes in storage devices like hoppers, cereal containers or salt shakers is rather incomplete even today [1–4]. The discharge of grains from storage devices is understood on an engineering level. Physical experiments for a fundamental understanding of these processes have been performed largely with spherical monodisperse hard grains.

Hoppers are common storage devices in agriculture. They make use of a unique property of granular matter: even though it consists of pieces of solid matter, it can flow out of the container outlet liquid-like, provided that the orifice is sufficiently large. In contrast to common liquids, which flow through outlets of any size provided that their surface tension is overcome by the pressure at the opening of the container, granular matter can produce clogs even when the outlet is much larger (approximately five times) than the individual particles. In the past six decades, numerous experimental studies, numerical simulations and theoretical modeling have been devoted to the statistical characterization of the discharge of such storage containers (e. g. Refs. [5–66]). Interesting aspects are, for example, the flow rates during discharge [5–21], clogging and jamming [22–30] flow in vibrated containers and the breaking of clogs by moving (oscillating or rotating) the orifice [31–42], shapes of blocking arches [43–47], packing and force chains [48–52], even silo collapse [53], obstacles near the orifice [54, 55, 66], gravity effects and submerged silos [56–58], and the roles of polydispersity, particle shapes [59–63] and softness [64,

This paper is dedicated to the memory of Robert P. Behringer.

This article is part of the Topical Collection: In Memoriam of Robert P. Behringer.

✉ Ralf Stannarius
ralf.stannarius@ovgu.de

Diego Sancho Martinez
diego.sancho@ovgu.de

Tilo Finger
tilo.finger@ovgu.de

Ellák Somfai
somfai.ellak@wigner.mta.hu

Tamás Börzsönyi
borzsonyi.tamas@wigner.mta.hu

[1] Institute of Physics, Otto von Guericke University, Magdeburg, Germany

[2] Institute for Solid State Physics and Optics, Wigner Research Center for Physics, Hungarian Academy of Sciences, Budapest, Hungary

65]. Most studies, with exception of the last two, have so far disregarded the role of softness of granular particles.

We note that it was Robert Behringer who achieved substantial progress in the identification of force chains in granular piles [30, 62, 67–69]. One of his important contributions was the visualization of force arches in clogged 2D silos filled with elliptical disks [62].

Soft grains exhibit very distinct features during the flow through narrow outlets. The hydrogel spheres studied by Hong et al. [64] and Ashour et al. [65] have very low friction coefficients (<0.03) and elastic moduli of the order of 50 kPa, which means they are deformed by the weight of overlying material at even moderate depths (few centimeters) below the granular bed surface. The particle volume thereby remains constant, the Poisson ratio is 1/2. The reported experiments with hydrogel spheres showed that these particles can pass much narrower orifices than frictional hard grains of comparable size without clogging. Hard spheres discharge freely only when the container outlet is roughly five times the particle diameter or larger, different equations for the clogging statistics as a function of the relative orifice sizes have been suggested [9, 28]. In contrast, the hydrogel spheres in a quasi-2D silo even pass orifices that are only two times as broad as their diameter, without forming permanent clogs. They exhibit a novel feature: transient clogs that resolve after a short stagnation of the flow. Similar non-permanent clogs occur with hard particles only under vibration [35]. Another striking observation in the hydrogel-filled container is that the pressure at the bottom does not saturate, but increases linearly (hydrostatically) with fill height [65]. The Janssen effect was not observed in the studied fill height range (maximum 80 cm). A striking consequence of this pressure characteristics is that the clogging statistics of the hydrogels becomes fill-height dependent. For a given orifice size, permanent clogs form when the pressure at the container bottom falls below a certain threshold. The smaller the outlet, the earlier clogging sets in.

There are yet more peculiarities of the investigated soft hydrogels: in the 2D silo, there are practically no stagnant zones, the complete content of the flat-bottomed container participates in the flow. Moreover, the flow profile at sufficiently large distance above the outlet level has rather plug-flow character, no lateral dependence of the vertical velocity [65].

A quasi-2D geometry (bin thickness of one or only few particle diameters) has an obvious advantage: it allows to monitor the particle arrangements and displacements in the container by optical observation (e. g. [65, 70]). However, it remains to be confirmed which of the results obtained in 2D bins can be generalized to 3D containers. In the latter, common non-invasive methods to monitor internal features and structures are X-ray Computed Tomography (XRCT) [71], Magnetic Resonance Imaging [72] and, with some limitations, optical scanning of particles in index-matched fluorescence labeled liquids [73]. In the present study, we use XRCT of stationary packings to map the local packing densities in the 3D container, and we employ image difference analysis to qualitatively reconstruct flow fields.

In previous experiments, we demonstrated the strength of XRCT for the mapping of orientational order and local packing fractions of non-spherical hard particles [47, 74]. Here, we use similar techniques to compare ensembles of soft particles with those of hard grains in 3D containers.

2 Experimental setup and materials

Soft monodisperse hydrogel spheres have been studied in the past by several researchers [64, 65, 69, 75–78]. Again, Robert Behringer's contribution to the characterization of soft sphere packings was substantial [69, 75, 78]: Refractive index matched scanning was employed to analyze packings of soft spheres suspended in a fluorescence labeled fluid [75, 78]. Using this technique, microscopic force imaging became possible. It allows the identification and quantitative characterization of the force chain networks in soft sphere packings [69].

The hydrogels studied in this work are distinctly different from the systems that were investigated earlier by means of optical scanning techniques: For the optical experiments, the hydrogels are immersed in an optical-density matched fluid [78], which has roughly the same mass density as the soft spheres. Buoyancy compensates the particle weight almost completely. In contrast, our hydrogel spheres, as well as those studied by Hong et al. [64], are in air. This has important consequences for the particle arrangements. As mentioned above, the weight of the overlying layers leads to an increasing pressure on the lower layers of the soft grains. These adopt their shapes so that they can pack much more efficiently than hard spheres in random as well as in regular packings.

We investigate hydrogel spheres of the same type as used earlier in a flat bin [65]. They were obtained in dry state from a commercial provider (*Happy Store*, Nanjing) and swelled in distilled water for at least 24 hours before using them. Between subsequent runs of the experiment, they were kept in distilled water. Immediately before the experiments, the excess water at their surfaces was wiped off and they were gravity-filled into the container. The container is a plastic bucket with a circular hole at the bottom (Fig. 1) that is kept close during filling.

The softness of the spheres has dramatic influence on the static pressure conditions, the characteristic discharge dynamics, as well as the flow field inside the silo during discharge. In combination with the low surface friction of

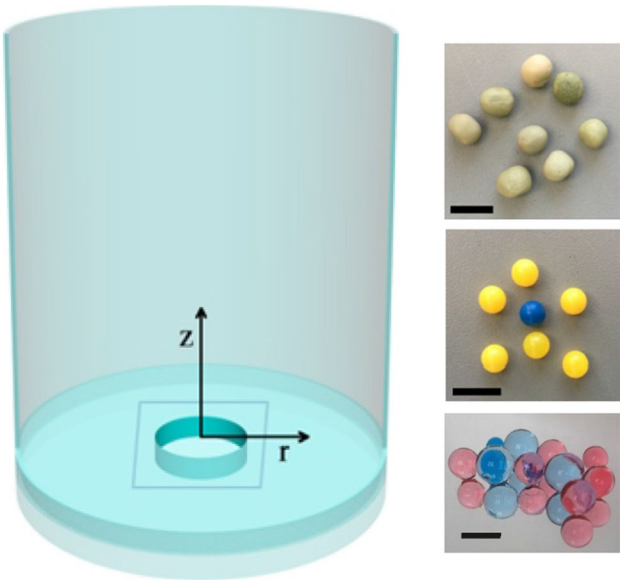

Fig. 1 Bin geometry and materials: we use a container of 19 cm diameter with an exchangeable bottom plate that allows us to vary the outlet diameter of a circular orifice in the center of the container bottom. The images at the side show the three investigated types of particles: peas with nearly spherical shapes, slightly polydisperse, diameters of 7.6 ± 0.3 mm; plastic spheres (airsoft bullets), monodisperse with 6 mm diameter, hydrogel spheres with diameter 9.2 ± 0.3 mm (the image shows a polydisperse mix, experiments were performed with monodisperse hydrogel spheres). Black bars represent 10 mm

the particles it leads to a fill-height dependent outflow characteristics, as observed in the flat container [65].

In a first set of experiments, we loaded the bucket with closed outlet stepwise with hydrogel spheres, so that tomograms could be recorded at different fill heights. The purpose of this part of the study was to determine the influence of the fill height (and consequently, the pressure) on the static packing of the soft spheres. We expect an increase of the packing fraction at the container bottom with increasing fill height, and also an increasing packing fraction towards the container bottom at a given fill height.

In the second part, the flow experiments, we started with the full container (approximately 7,000 hydrogel spheres). The outlet was then opened and we let a few (12 ± 2) particles run through the orifice. Then we closed it again and took a full 3D tomographic image. Thereafter, we repeated this controlled discharge multiple times. Typically, 40 tomograms were recorded for each material. For comparison and benchmark purposes, we also performed similar outflow experiments with hard grains (see below). The purpose of that part of the study was to compare the flowing regions and to identify stagnant zones in both soft and hard spherical granular materials.

The tomographic images were recorded with the robot-based flat panel X-ray C-arm system *Siemens Artis zeego* of the STIMULATE-lab, Otto von Guericke University, Magdeburg. The spacial resolution was approximately 2 pixel/mm, recorded volumes are 25.2 cm × 25.2cm × 19 cm. We employed different techniques to extract the desired information from the tomograms. In the static packing fraction measurements, we identified each sphere by means of image analysis. Then, the local packing fraction could be determined from the positions of the centers of mass of all spheres and the average radius of the spheres. Even if the hydrogel spheres are slightly polydisperse, with a radius variation by a few percent, this method gives an overall reliable vertical profile of the packing fractions since there is no size segregation during filling, and statistically the spheres in each layer have the same average nominal diameter.

The evaluation of the flow profile was performed by comparison of subsequent tomograms before and after a controlled discharge. The total amount of material released between the tomograms corresponds to a horizontal layer of a thickness much less than the particle diameter. Thus, most of the particles can be collated in subsequent tomograms. Figure 2 shows two typical vertical cross sections of tomographic images, in the center of the container (see sketch).

Here, we labeled differences between two subsequent tomograms in red color. Flowing regions appear in red, stagnant regions in a green background hue. The images already give a qualitative impression of the flowing and stagnant zones, which differ substantially for the soft and hard materials. Because of axial symmetry of the experimental geometry, all vertical planes containing the central axis are equivalent and show similar features. A more detailed discussion is found in Sect. 3.2 where we describe a more quantitative method to evaluate the dynamics of the grains.

3 Experiment and data analysis

3.1 Packing of soft spheres

Before describing the different dynamic behavior of soft and hard grains, we first explore the static properties of the packings in the container. After the gravitational filling, we expect a random packing of the spheres in the bin that is quite similar to the so-called 'poured random packing'. For hard spheres, the filling fraction of such configurations is somewhere between 0.61 and 0.635, but never larger than 0.64 even when the ensemble is compacted by shaking [79]. For soft spheres, this value depends both on the elastic properties of the spheres and the local pressure. As we have shown earlier, the pressure in a granular bed formed by hydrogel spheres in a 2D container increases nearly linearly with depth. Since the spheres pack more efficiently under

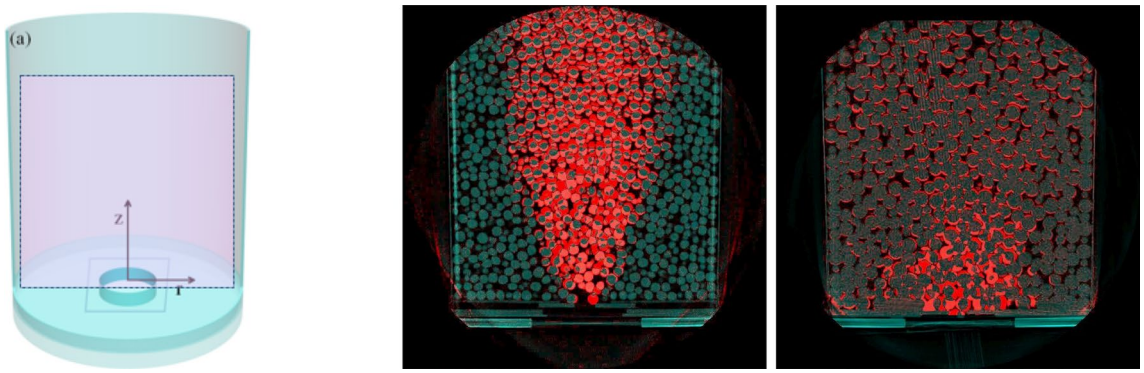

Fig. 2 Differences of X-ray tomogram slices before and after the discharge of a small avalanche (≈ 12 grains). The sketch to the left visualizes the geometry and the position of the two slices. The two images were obtained for hard peas (left) and soft hydrogel spheres (right). The green color channel is a positive superposition (addition) of the two images, the red channel gives the absolute value of the differences. The images allow to identify the zones where particles move

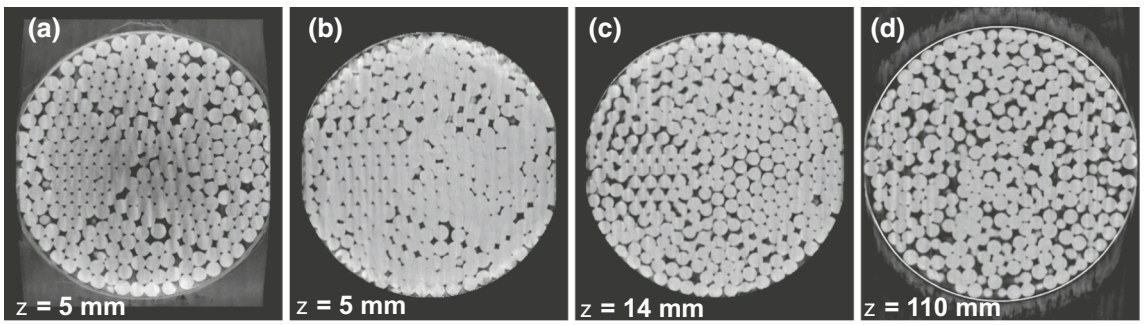

Fig. 3 Horizontal cross sections of tomograms of the hydrogel-sphere filled container. **a** $z = 5$ mm (approximately 1 sphere radius) above the bottom, fill height 22 mm, **b** $z = 5$ mm above bottom, fill height 180 mm, water that seeped down from the overlying spheres has partially filled some voids, **c**) $z = 14$ mm above bottom, fill height 180 mm, all spheres dry and clearly distinguishable, surface-induced layering, **d**) $z = 110$ mm above bottom, fill height 180 mm, random packing, layering only near side walls

higher pressure, we expect the packing fraction in the container to be height dependent. The pressure at the bottom of a 10 cm high bed is approximately 800 Pa (assuming 80 % fill fraction and the density of the hydrogel spheres being almost exactly equal to the density of water). An individual sphere at the bottom is then exposed to a force of the order of 0.7 N. With an elastic modulus of approximately 50 kPa, Hertzian contacts between such two spheres at the container bottom will then have diameters of up to 6 mm, the spheres flatten on average by up to 0.3 mm at each contact. Consequently, the fill fraction will be substantially larger than for randomly packed *hard* spheres. We calculated the static packing quantitatively as a function of the container fill height by identifying each hydrogel sphere in the tomogram. This was possible except in the tomograms of the largest fill heights ($h > 150$ mm) where a noticeable amount of water accumulated in the bottom layer (see Fig. 3b), so that not all individual spheres could be identified unambiguously.

Figure 3 shows some exemplary cuts of the tomograms, (a) is the cut in the middle of the bottom layer, demonstrating the quality of the XRCT images. The fill level is slightly more than 2 layers of spheres. Each sphere can be clearly identified and the position can be determined. (b) shows the same level in a container filled to a height of 18 cm. Some water has seeped down from the overlying spheres and partially filled the voids. Even though this leakage is well below 1 % of the total hydrogel volume, the water masks the voids in the bottom layer and frustrates the identification of all spheres. (c) is a cut in the same tomogram 1.5 particle diameters above the bottom. There, no leaked water is present and the separation of grains is unambiguously possible. (d) shows a cut of a typical randomly packed soft spheres arrangement, with a local packing fraction ϕ of about 0.78.

The packing fraction in all tomograms was found to be much larger than 0.7 everywhere, except directly below the surface (1–2 particle diameters deep) and except in the layered structures induced by the flat bottom. This layer structure extends approximately four particle diameters deep into the container. The average packing fraction deep in the granular bed reaches approximately 0.78 (Fig. 4). A

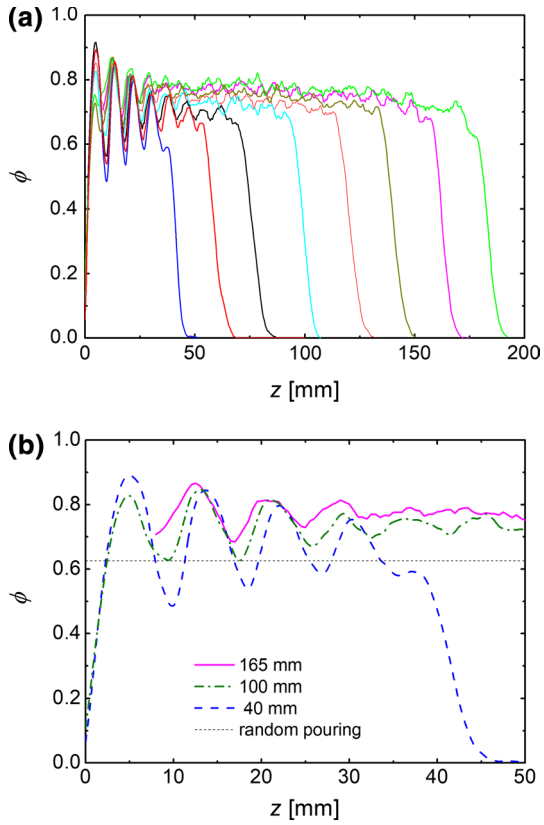

Fig. 4 Packing fractions determined from XRCT images. **a** Vertical profiles of $\phi(z)$ above the bottom at $z = 0$ at different fill heights of the container. The assignment of the individual graphs can be made directly from the drop of $\phi(z)$ at the upper surface of the granular bed. **b** zoom into the first layers above the bottom plate. For the largest fill height shown, 165 mm, the first layer above the bottom plate contains some free water (cf. Fig. 3b), thus the packing fraction could not be determined unambiguously

rough estimate of the effect of deformation of the particles under the weight of the overlying material can be obtained as follows: Let us assume that the grains in 10 cm depth are compressed in the direction of the contacts by about 6 % of their radius (see above), then, the filling fraction raises to roughly 1.2 times that of hard spheres, viz. about 73 to 76 %. The remaining few % may result from a more efficient adaption of the soft spheres to the surrounding cages formed by neighbors.

Figure 4b shows a zoomed view of the packing fraction characteristics $\phi(z)$ near the bottom. It is evident that the bottom layers themselves are increasingly compressed with increasing fill height (higher pressure), and that the modulation depth is smaller for larger fill heights. Figure 5 shows photographs of hydrogel spheres near the wall of a transparent container with flat walls. It shows the bottom layers of a container filled to a height of ≈ 28 mm (a) and 100 mm (b). The contact areas reflect the pressures acting on each sphere. In principle, one can evaluate such pictures to identify the forces and the structure of the force chain network near the side walls. Diameters of the contact areas are larger for high fill levels because of the increased pressure at the bottom. The observed indentations are in reasonable agreement with expected contact forces for the estimated pressures and known elastic moduli.

We note that the 'random pouring' fill fractions determined in this sections apply only to freshly filled containers. After material has flown out of the bottom outlet, the packing fraction changes everywhere except in the stagnant zones. The granulate dilates in the flowing zones, not only during discharge. Even in the clogged states, the packing fraction remains lower in the regions that have participated in the discharge. This will be analyzed in more detail in the next section.

3.2 Flow profiles

The dynamic behavior of soft grains is even more distinctive than their static properties. Figure 2 already gave a qualitative impression of the peculiar flow characteristics in the silo. For a more quantitative evaluation, we compared 40 individual tomograms recorded during controlled stepwise discharge of the container as described in Sect. 2. An image difference analysis was performed for all 39 discharges. A threshold was set to binarize each voxel in the tomograms

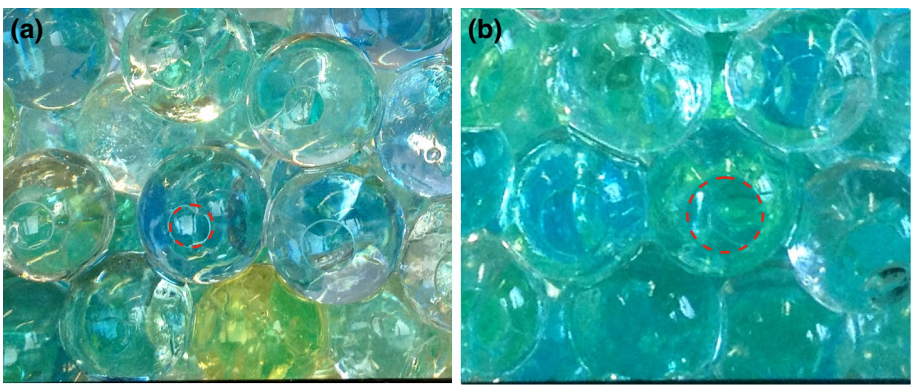

Fig. 5 Bottom layers of hydrogel spheres at the walls of a glass container filled to a total height of ≈ 28 mm (**a**) and 100 mm (**b**). The contact areas with the glass walls can be easily identified. They reflect the deformations of the spheres by Hertzian contacts. Exemplary contacts of 2.8 mm (**a**) and 5 mm (**b**) diameter are marked by dashed circles. Image sizes are 30×25 mm^2

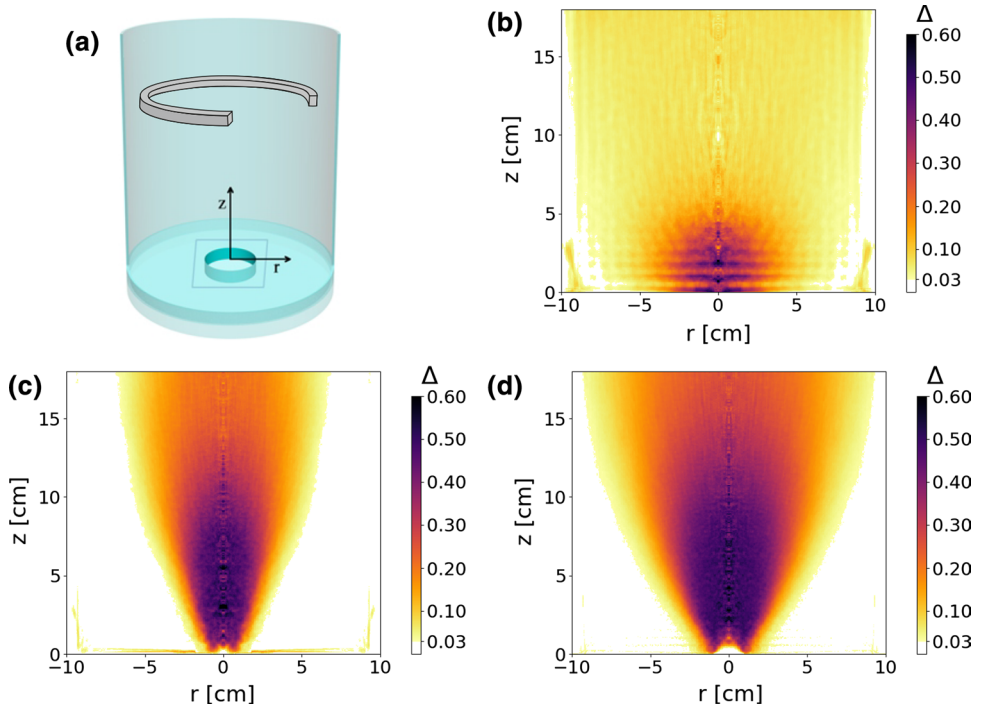

Fig. 6 Averages of the differences of subsequent X-ray tomogram pairs before and after small discharges of few grains. **a** Sketch of the ring-shaped regions that are averaged to obtain geometrically equivalent positions: **b** hydrogel spheres flow everywhere in the container. Hard grains flow only in funnel-shaped regions: **c** for peas the aperture is about $2 \times 20°$, and **d** for airsoft bullets somewhat wider, about $2 \times 29°$. Outside these funnels, the material is at rest (image differences smaller than a threshold value of 0.03 are displayed in white). Well above the orifice (approximately one container radius above) the soft sphere flow is rather uniform in each horizontal plane, it has plug flow character. Fluctuations near the central axis are artifacts, because averaging is there only over one and the same particle in the center. Color bars refer to the averaged voxel differences Δ (see text), which for small Δ are proportional to the outflow velocity. For better clarity, each image is mirrored at the central axis

as hydrogel (1) or air (0) with Otsu's method [80]. Then, we computed the absolute differences of voxels of subsequent tomograms. The two limits of the averaged differences Δ are zero when there is no flow and thus no change in the voxel, and 1/2 if the flow is so fast that the voxel content changes randomly between both states.[1] When the displacement of the grains is on average smaller than half the grain diameter (cf. Fig. 2), the relation between the averaged image difference and the flow velocity can be assumed to be linear in first approximation.

The obtained data were averaged twofold: First, we averaged over all geometrically equivalent positions in the cylindrical container, i. e. all positions with equal height above outlet and equal radial distance from the cylinder axis (see sketch in Fig. 6a). This is justified by the premise that, on average, no distinguished azimuthal direction exists in the geometry of the experiment, and the flow field is on average axially symmetric. Second, we average all differences between subsequent images to obtain a time-averaged magnitude of the flow field. The results are shown for the three particle types in Fig. 6b–d. In the hydrogel experiments, each discharge consisted of approximately 12 spheres, then flow was stopped manually by closing the outlet. In the experiment with peas, the flow through the 15 mm diameter orifice clogged spontaneously after avalanches with mean size of 25 peas. In the airsoft ammunition experiments (19 mm orifice), spontaneous clogs occurred after avalanches with a mean size of 50 grains.

We have to keep in mind that the flow field data obtained from static tomograms are merely qualitative, because the durations of the discharges were not measured, and finally, because the number of discharged grains between two tomograms was not exactly counted, and because the relation between the image differences and the actual local flow rate was not determined quantitatively. It is clear that stronger flow leads to larger differences in the tomograms, but the relation does not need to be linear. As described above, we can assume linearity only for small displacements, smaller than the particle radii, between subsequent images. This condition was fulfilled in all experiments. Also, the

[1] When averaging finite ensembles, the maximum value of Δ can even become slightly larger than 1/2 due to noise.

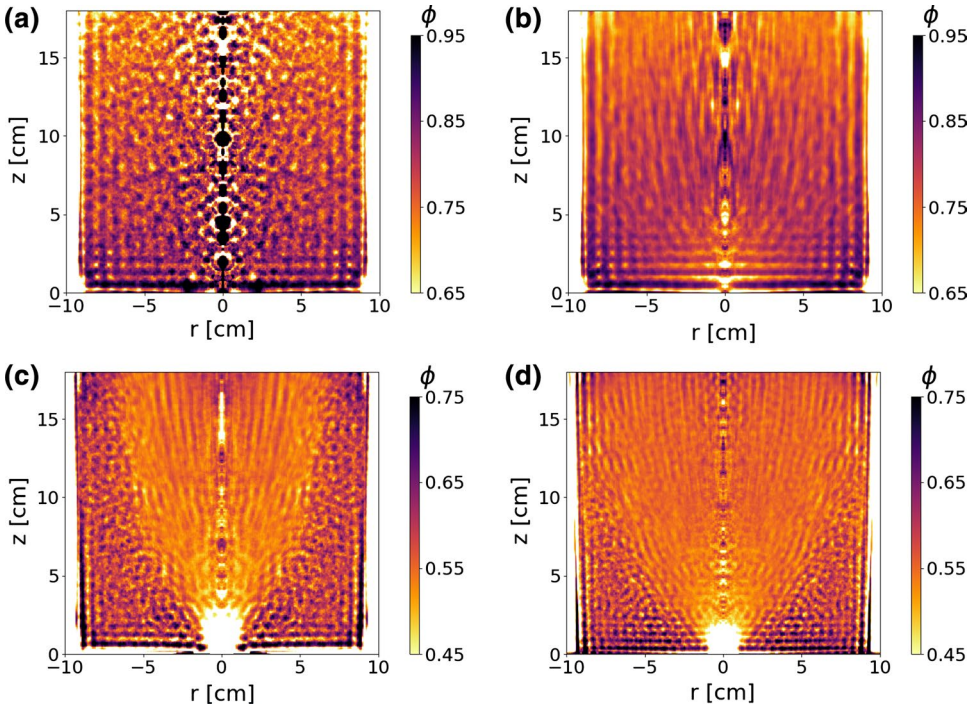

Fig. 7 Averaged cross-sections of X-ray tomograms providing the local packing fractions: **a** hydrogel spheres after first filling of the container (single realization); and **b**–**d** averages of 30-40 clogged states: **b** hydrogel spheres, **c** peas, and **d** airsoft bullets. The soft spheres have higher packing fraction near the bottom due to larger pressure, but after the discharge of grains there is a particle density drop near the outlet (**b**). For hard particles, the funnel-shaped flowing zone has clearly lower packing density. Note that the color scale for the hydrogels is different from that of the hard particles. The averaging over equivalent locations was performed in the same way as in Fig. 6. Again, the fluctuations near the central axis are artifacts, because spatial averaging is there over one and the same particle in the center; this is especially prominent in (**a**) displaying a single realization. For better clarity, the images are mirrored at the central axis

evaluation method disregards the local direction of the flow field, considering only the absolute displacements of individual grains.

Nevertheless, Fig. 6 provides a good picture of the flowing zone geometry inside the 3D bins. It is obvious that the hard spheres (peas, airsoft bullets) form a funnel-like channel with large stagnant regions near the container wall. It is reasonable to assume that the funnel finally reaches the bin walls at some height above the outlet, but this is far above our container top.

The tomograms can also be used to obtain the static local packing fractions in the bin. This is seen in Fig. 7, where instead of the absolute differences, we *summed up* the binarized tomograms for averaging. There is a clear difference in the arrangements of hard and soft grains. First, the packing fraction is much higher for the soft spheres, this was already discussed in Sect. 3.1. But moreover, one can clearly identify the reduced packing fractions in the flowing zones of the hard grains. This is a consequence of shear dilatancy [47] in the flow zones. The packing fraction drops by roughly 10 %. The boundaries between the flowing and stagnant zones are sharp and clearly distinguished, as in Fig. 6.

In contrast, the soft grains show a more or less unstructured packing profile, except for the induced layering at the walls. This is partly due to the geometry of the flow which involves all parts of the container interior, but it may also be a consequence of a much less pronounced shear dilatancy. The mean local packing fraction of the soft spheres after discharge of material does hardly differ from the initial packing after filling the bin. The loss of structural details in Fig. 7b with respect to Fig. 7a occurs only because the latter is computed from a single tomogram, the former is an average of 39 tomograms. This property has not been studied for soft granular matter so far, even though shear experiments with hydrogel spheres have been reported [69, 75, 78]. There is a slight drop in packing fraction immediately above the outlet.

All tomograms show a pronounced layering of the material at the bottom and side walls. It is less developed in the peas ensemble presumably because these grains are not exactly monodisperse. It is well developed both for the monodisperse hard airsoft bullets and for the soft hydrogels. The layering there exists even though all grains are moved during the discharges. Another prominent

characteristics of the hydrogel spheres is the above-described height dependence of the packing fraction.

4 Conclusions and summary

In previous experiments with soft, nearly frictionless hydrogel spheres, it was found that in a quasi-2D container both the pressure distribution and the outflow characteristics are substantially different from the case of frictional hard grains. Here, we have shown that several of these observations can be generalized to 3D containers: The pressure increases roughly linearly with fill height of the container, leading to a more efficient packing of the soft grains compared to hard spheres. The 'random-pouring' packing fraction approaches a value of $\phi \approx 0.78$ already a few layers below the granular bed surface. The compression of the hydrogel at Hertzian contacts can be used to measure pressures and force chain networks even quantitatively, as it was suggested for hydrogels in neutrally buoyant fluids under external forcing. The flowing regions during discharge extend over the whole interior of the container in the 3D geometry, as well as in the flat quasi-2D bin. In the 2D experiment [65], the observed hexagonal packing may be partially responsible for the plug-flow character of the velocity field inside the bin. In the 3D container, there is no crystalline packing of the soft spheres but the flow is still plug-flow like in sufficient distance from the outlet. For a full understanding of the above-described dynamic phenomena, the effects of softness and low friction still need to be discriminated. We hypothesize that a combination of both features is responsible for the observed dynamical properties. Further experiments with high-friction soft grains and low-friction rigid grains may provide the answers.

The XRCT data contain further valuable information on distances between neighbors in the soft sphere packings, on contact numbers and orientational distributions of force chains. These evaluations are the subject of ongoing work.

Finally, we note that the employed experimental technique did not allow to record real time data during the outflow. Therefore, it remains to be demonstrated that continuous outflow has the same qualitative features as the pulsed flow present in this study. For that purpose, experiments with high-speed tomography (1000 two-dimensional slices per second in a 3D container) are under way with ROFEX at the Helmholtz Center Rossendorf. Preliminary results support the 3D observations from the present pulsed-flow study qualitatively.

Acknowledgements We thank Torsten Trittel for valuable technical assistance. Tivadar Pongó and Maja Illig are acknowledged for participating in the measurements. The authors acknowledge financial support by DAAD and TEMPUS within the researcher exchange program (Grant No. 274464) and by the Hungarian National Research, Development and Innovation Office NKFIH under Grant OTKA K 116036. Georg Rose and Cindy Lübeck are cordially acknowledged for their assistance and for the opportunity to use the X-ray tomograph in the STIMULATE lab.

Compliance with ethical standards

Conflict of interest The authors declare that there is no conflict of interest.

References

1. Jaeger, H.M., Nagel, S.R., Beringer, R.P.: Granular solids, liquids, and gases. Rev. Mod. Phys. **68**, 1259 (1996)
2. de Gennes, P.G.: Granular matter: a tentative view. Rev. Mod. Phys. **71**, S374 (1999)
3. Campbell, C.S.: Granular material flows—An overview. J. Powder Techn. **162**, 208 (2006)
4. Radjai, F., Roux, J.N., Daouadji, A.: Modeling granular materials: century-long research across scales. J. Eng. Mech. **143**(4), 04017002 (2017)
5. Franklin, F.C., Johanson, L.N.: Flow of granular material through a circular orifice. Chem. Eng. Sci. **4**, 119 (1955)
6. Beverloo, W.A., Leniger, H.A., Van de Velde, J.J.: The flow of granular solids through orifices. Chem. Eng. Sci. **15**, 260 (1961)
7. Neddermann, R.M., Tuzun, U., Savage, S.B., Houlsby, G.T.: The flow of granular materials I: discharge rates from hoppers. Chem. Eng. Sci. **37**, 1597 (1982)
8. Chang, C.S., Converse, H.H., Steele, J.L.: Flow rates of grain through various shapes of vertical and horizontal orifices. Trans. Am. Soc. Agric. Eng. **34**, 1789 (1991)
9. Zuriguel, I., et al.: Jamming during the discharge of granular matter from a silo. Phys. Rev. E **71**, 051303 (2005)
10. To, K.: Jamming transition in two-dimensional hoppers and silos. Phys. Rev. E **71**, 060301 (2005)
11. Mankoc, C., Janda, A., Arévalo, R., Pastor, J.M., Zuriguel, I., Garcimartín, A., Maza, D.: The flow rate of granular materials through an orifice. Granul. Matter **9**, 407 (2007)
12. Mankoc, C., Janda, A., Arévalo, R., Pastor, J.M., Zuriguel, I., Garcimartín, A., D, M.: The flow rate of granular materials through an orifice. Granul. Matter **9**, 407 (2007)
13. Hilton, J.E., Cleary, P.W.: Granular flow during hopper discharge. Phys. Rev. E **84**, 011307 (2011)
14. Garcimartín, A., Zuriguel, I., Janda, A., Maza, D.: Fluctuations of grains inside a discharging two-dimensional silo. Phys. Rev. E **84**, 031309 (2011)
15. Uñac, R.O., Vidales, A.M., Benegas, O.A., Ippolito, I.: Experimental study of discharge rate fluctuations in a silo with different hopper geometries. Powder Technol. **225**, 214 (2012)
16. Masuda, T., Nishinari, K., Schadschneider, A.: Critical bottleneck size for jamless particle flows in two dimensions. Phys. Rev. Lett. **112**, 138701 (2014)
17. Benyamine, M., Djermane, M., Dalloz-Dubrujeaud, B., Aussillous, P.: Discharge flow of a bidisperse granular media from a silo. Phys. Rev. E **90**, 032201 (2014)
18. Janda, A., Harich, R., Zuriguel, I., Maza, D., Cixous, P., Garcimartin, A.: Unjamming a granular hopper by vibration. Phys. Rev. E **79**, 031302 (2009)
19. Sheldon, H.G., Durian, D.J.: Granular discharge and clogging for tilted hoppers. Granul. Matter **12**, 579 (2010)
20. Saraf, S., Franklin, S.V.: Power-law flow statistics in anisometric (wedge) hoppers. Phys. Rev. E **83**, 030301 (2011)

21. Hirshfeld, D., Rapaport, D.C.: Granular flow from a silo: discrete-particle simulations in three dimensions. Eur. Phys. J. E **4**, 193 (2001)
22. To, K., Lai, P.Y., Pak, H.K.: Jamming of granular flow in a two-dimensional hopper. Phys. Rev. Lett. **86**, 71 (2001)
23. Manna, S.S., Herrmann, H.J.: Intermittent granular flow and clogging with internal avalanches. Eur. Phys. J. E **1**, 341 (2000)
24. Zuriguel, I., Pugnaloni, L.A., Garcimartín, A., Maza, D.: Jamming during the discharge of grains from a silo described as a percolating transition. Phys. Rev. E **68**, 030301 (2003)
25. Janda, A., Zuriguel, I., Garcimartín, A., Pugnaloni, L.A., Maza, D.: Jamming and critical outlet size in the discharge of a two-dimensional silo. EPL **84**, 44002 (2008)
26. Zuriguel, I.: Clogging of granular materials in bottlenecks. P. Phys. **6**, 060014 (2014)
27. Zuriguel, I., et al.: Clogging transition of many-particle systems flowing through bottlenecks. Sci. Rep. **4**, 7324 (2014)
28. Thomas, C.C., Durian, D.J.: Geometry dependence of the clogging transition in tilted hoppers. Phys. Rev. E **87**, 052201 (2013)
29. Thomas, C.C., Durian, D.J.: Fraction of clogging configurations sampled by granular hopper flow. Phys. Rev. Lett. **114**, 178001 (2015)
30. Tang, J., Behringer, R.P.: How granular materials jam in a hopper. Chaos **21**, 041107 (2011)
31. Nowak, E.R., Knight, J.B., Ben-Naim, E., Jaeger, H.M., Nagel, S.R.: Density fluctuations in vibrated granular materials. Phys. Rev. E **57**, 1971 (1998)
32. Hunt, M.L., Weathers, R.C., Lee, A.T., Brennen, C.E., Wassgren, C.R.: Effects of horizontal vibration on hopper flows of granular materials. Phys. Fluids **11**, 1 (1999)
33. Wassgren, C.R., Hunt, M.L., Freese, P.J., Palamara, J., Brennen, C.E.: Effects of vertical vibration on hopper flows of granular material. Phys. Fluids **14**, 10 (2002)
34. Chen, K., Stone, M.B., Barry, R., Lohr, M., McConville, W., Klein, K., Sheu, B.L., Morss, A.J., Scheidemantel, T., Schiffer, P.: Flux through a hole from a shaken granular medium. Phys. Rev. E **74**, 011306 (2006)
35. Mankoc, C., Garcimartín, A., Zuriguel, I., Maza, D., Pugnaloni, L.A.: Role of vibrations in the jamming and unjamming of grains discharging from a silo. Phys. Rev. E **80**, 011309 (2009)
36. Janda, A., Maza, D., Garcimartín, A., Kolb, E., Lanuza, J., Clément, E.: Unjamming a granular hopper by vibration. Europhys. Lett. **87**, 24002 (2009)
37. Mankoc, C., Garcimartín, A., Zuriguel, I., Maza, D., Pugnaloni, L.A.: Role of vibrations in the jamming and unjamming of grains discharging from a silo. Phys. Rev. E **80**, 011309 (2009)
38. Lozano, C., Lumay, G., Zuriguel, I., Hidalgo, R.C., Garcimartín, A.: Breaking arches with vibrations: the role of defects. Phys. Rev. Lett. **109**, 068001 (2012)
39. Arévalo, R., Zuriguel, I., Maza, D., Garcimartín, A.: Role of driving force on the clogging of inert particles in a bottleneck. Phys. Rev. E **89**, 042205 (2014)
40. Lozano, C., Zuriguel, I., Garcimartín, A.: Stability of clogging arches in a silo submitted to vertical vibrations. Phys. Rev. E **91**, 062203 (2015)
41. To, K., Tai, H.T.: The sands of time run faster near the end. Phys. Rev. E **96**, 032906 (2017)
42. To, K., Mo, Y.K., Huang, J.R.: Granular flow from silos with rotating orifice. arXiv:1902:00393 (2019)
43. Drescher, A., Waters, A.J., Rhoades, C.A.: Arching in hoppers: II. Arching theories and critical outlet size. Powder Technol. **84**, 177 (1995)
44. Garcimartín, A., Zuriguel, I., Pugnaloni, L.A., Janda, A.: Shape of jamming arches in two-dimensional deposits of granular materials. Phys. Rev. E **82**, 031306 (2010)
45. Oldal, I., Keppler, I., Csizmadia, B., Fenyvesi, L.: Outflow properties of silos: the effect of arching. Adv. Powder Tech. **23**, 290 (2012)
46. Rubio-Largo, S.M., Janda, A., Maza, D., Zuriguel, I., Hidalgo, R.C.: Disentangling the free-fall arch paradox in silo discharge. Phys. Rev. Lett. **114**, 238002 (2015)
47. Börzsönyi, T., Somfai, E., Szabó, B., Wegner, S., Mier, P., Rose, G., Stannarius, R.: Packing, alignment and flow of shape-anisotropic grains in a 3D silo experiment. New J. Phys. **18**, 093017 (2016)
48. Uñac, R., Vidales, A., Pugnaloni, L.: The effect of the packing fraction on the jamming of granular flow through small apertures. J. Stat. Mech.: Theor. Exp. **04**, P04008 (2012)
49. Hidalgo, R.C., Lozano, C., Zuriguel, I., Garcimartín, A.: Force analysis of clogging arches in a silo. Granul. Matter **15**, 841 (2013)
50. Aguirre, M.A., De Schant, R., Géminard, J.-C.: Granular flow through an aperture: influence of the packing fraction. Phys. Rev. E **90**, 012203 (2014)
51. Wang, Y., Lu, Y., Ooi, J.Y.: A numerical study of wall pressure and granular flow in a flat-bottomed silo. Powder Technol. **282**, 43 (2015)
52. Grudzien, K., Niedostatkiewicz, M., Adrien, J., Tejchman, J., Maire, E.: Quantitative estimation of volume changes of granular materials during silo flow using X-ray tomography. Chem. Eng. Proc.: Process Intensif. **50**(1), 59 (2011)
53. Gutiérrez, G., Colonnello, C., Boltenhagen, P., Darias, J.R., Peralta-Fabi, R., Brau, F., Clément, E.: Silo collapse under granular discharge. Phys. Rev. Lett. **114**, 018001 (2015)
54. Zuriguel, I., et al.: Silo clogging reduction by the presence of an obstacle. Phys. Rev. Lett. **107**, 278001 (2011)
55. Lozano, C., Janda, A., Garcimartín, A., Maza, D., Zuriguel, I.: Flow and clogging in a silo with an obstacle above the orifice. Phys. Rev. E **86**, 031306 (2012)
56. Dorbolo, S., et al.: Influence of the gravity on the discharge of a silo. Granul. Matter **15**, 263 (2013)
57. Arévalo, R., Zuriguel, I.: Clogging of granular materials in silos: effect of gravity and outlet size. Soft Matter **12**, 123 (2016)
58. Wilson, T.J., Pfeifer, C.R., Meysingier, N., Durian, D.J.: Granular discharge rate for submerged hoppers. P. Phys. **6**, 060009 (2014)
59. Jin, B., Tao, H., Zhong, W.: Flow behaviors of non-spherical granules in rectangular hopper. Chin. J. Chem. Eng. **18**, 931 (2010)
60. Tao, H., Jin, B., Zhong, W., Wang, X., Ren, B., Zhang, Y., Xiao, R.: Discrete element method modeling of non-spherical granular flow in rectangular hopper. Chem. Eng. Process.: Process Intensif. **49**, 151 (2010)
61. Lozano, C., Zuriguel, I., Garcimartín, A., Mullin, T.: Granular segregation driven by particle interactions. Phys. Rev. Lett. **114**, 178002 (2015)
62. Tang, J., Behringer, R.P.: Orientation, flow, and clogging in a two-dimensional hopper: ellipses vs disks. Europhys. Lett. **114**, 34002 (2016)
63. Ashour, A., Wegner, S., Trittel, T., Börzsönyi, T., Stannarius, R.: Outflow and clogging of shape-anisotropic grains in hoppers with small apertures. Soft Matter **13**, 402 (2017)
64. Hong, X., Kohne, M., Morrell, M., Wang, H.R., Weeks, E.R.: Clogging of soft particles in two-dimensional hoppers. Phys. Rev. E **96**, 062605 (2017)
65. Ashour, A., Trittel, T., Börzsönyi, T., Stannarius, R.: Silo outflow of soft frictionless spheres. Phys. Rev. Fluids **2**, 123302 (2017)
66. Garcimartín, A., Pastor, J.M., Ferrer, L.M., Ramos, J.J., Martín-Gómez, C., Zuriguel, I.: Flow and clogging of a sheep herd passing through a bottleneck. Phys. Rev. E **91**, 022808 (2015)
67. Howell, D., Behringer, R.P., Veje, C.: Stress fluctuations in a 2D granular couette experiment: a continuous transition. Phys. Rev. Lett. **82**, 5241 (1999)

68. Majmudar, T.S., Behringer, R.P.: Contact force measurements and stress-induced anisotropy in granular materials. Nature **435**, 1079 (2005)
69. Brodu, N., Dijksman, J.A., Behringer, R.P.: Spanning the scales of granular materials through microscopic force imaging. Nat. Comm. **6**, 6361 (2015)
70. Szabó, B., Kovács, Z., Wegner, S., Ashour, A., Fischer, D., Stannarius, R., Börzsönyi, T.: Flow of anisometric particles in a quasi-two-dimensional hopper. Phys. Rev. E **97**, 062904 (2018)
71. Weis, S., Schröter, M.: Analyzing X-ray tomographies of granular packings. Rev. Sci. Instr. **88**, 051809 (2017)
72. Stannarius, R.: Magnetic resonance imaging of granular materials. Rev. Sci. Instr. **88**, 051806 (2017)
73. Dijksman, J.A., Brodu, N., Behringer, R.P.: Refractive index matched scanning and detection of soft particles. Rev. Sci. Instr. **88**, 051807 (2017)
74. Wegner, S., Stannarius, R., Boese, A., Rose, G., Szabo, B., Somfai, E., Börzsönyi, T.: Effects of grain shape on packing and dilatancy of sheared granular materials. Soft Matter **10**, 5157 (2014)
75. Dijksman, J.A., Zheng, H., Behringer, R.P.: Imaging soft sphere packings in a novel triaxial shear setup. AIP Conf. Proc. **1542**, 457 (2013)
76. Bertrand, T., Peixinho, J., Mukhopadhyay, S., MacMinn, C.W.: Dynamics of swelling and drying in a spherical gel. Phys. Rev. Appl. **6**(6), 064010 (2016)
77. Hong, X., Kohne, M., Weeks, E.R.: Clogging of soft particles in 2D hoppers. arXiv: 1512.02500v2 (2016)
78. Dijksman, J.A., Brodu, N., Behringer, R.P.: Refractive index matched scanning and detection of soft particles. Rev. Sci. Instrum. **88**, 051807 (2017)
79. Torquato, S., Truskett, T.M., Debenedetti, P.G.: Is random close packing of spheres well defined? Phys. Lev. Lett. **84**, 2064 (2000)
80. Otsu, N.: Influence of particle shape and surface friction variability on response of rod-shaped particulate media. IEEE Trans. Syst. Man Cybern. **SMC–9**, 62 (1979)